OPEN

PRS GLOBAL OPEN EXPERIMENTAL

A Novel Reticular Dermal Graft Leverages Architectural and Biological Properties to Support Wound Repair

Anouska Dasgupta, PhD*
Dennis Orgill, MD, PhD†‡
Robert D. Galiano, MD§
Charles M. Zelen, DPM¶
Yen-Chen Huang, PhD*
Evangelia Chnari, PhD*
William W. Li, MD‖

Background: Acellular dermal matrices (ADMs) are frequently used in reconstructive surgery and as scaffolds to treat chronic wounds. The 3-dimensional architecture and extracellular matrix provide structural and signaling cues for repair and remodeling. However, most ADMs are not uniformly porous, which can lead to heterogeneous host engraftment. In this study, we hypothesized that a novel human reticular ADM (HR-ADM; AlloPatch Pliable, Musculoskeletal Transplant Foundation, Edison, N.J.) when aseptically processed would have a more open uniform structure with retention of biological components known to facilitate wound healing.

Methods: The reticular and papillary layers were compared through histology and scanning electron microscopy. Biomechanical properties were assessed through tensile testing. The impact of aseptic processing was evaluated by comparing unprocessed with processed reticular grafts. In vitro cell culture on fibroblasts and endothelial cells were performed to showcase functional cell activities on HR-ADMs.

Results: Aseptically processed HR-ADMs have an open, interconnected uniform scaffold with preserved collagens, elastin, glycosaminoglycans, and hyaluronic acid. HR-ADMs had significantly lower ultimate tensile strength and Young's modulus versus the papillary layer, with a higher percentage elongation at break, providing graft flexibility. These preserved biological components facilitated fibroblast and endothelial cell attachment, cell infiltration, and new matrix synthesis (collagen IV, fibronectin, von Willebrand factor), which support granulation and angiogenic activities.

Conclusions: The novel HR-ADMs provide an open, interconnected scaffold with native dermal mechanical and biological properties. Furthermore, aseptic processing retains key extracellular matrix elements in an organized framework and supports functional activities of fibroblasts and endothelial cells. *(Plast Reconstr Surg Glob Open 2016;4:e1065; doi: 10.1097/GOX.0000000000001065; Published online 4 October 2016.)*

Acellular dermal matrices (ADMs) are commonly used in wound healing and tissue repair to facilitate wound closure and regenerative remodeling.[1–3] The extracellular matrix (ECM), a major component of ADMs, provides structure, cell-signaling cues, and mechanical support to facilitate the healing process.[4–8] Key dermal ECM components include collagens, elastin, glycosaminoglycans (GAGs), and hyaluronic acid (HA).[4,9–11] The ECM

*From the *Musculoskeletal Transplant Foundation, Edison, N.J.; †Department of Surgery, Brigham and Women's Hospital, Boston, Mass.; ‡Department of Surgery, Harvard Medical School, Boston, Mass.; §Division of Plastic Surgery, Northwestern University Feinberg School of Medicine, Chicago, Ill.; ¶Professional Education and Research Institute, Roanoke, Va.; and ‖The Angiogenesis Foundation, Cambridge, Mass.*

Received for publication February 12, 2016; accepted August 10, 2016.

DOI: 10.1097/GOX.0000000000001065

Disclosure: *Dennis P. Orgill, MD, PhD, is a consultant for MTF and receives research funding through grants to Brigham and Women's Hospital. Robert D. Galiano, MD, is a consultant for MTF and receives research funding through grants to Northwestern University School of Medicine. Charles M. Zelen, DPM, is employed by the Professional Education and Research Institute, for which he is a medical director and CEO; funds have been received from MTF to conduct clinical trials. The other authors have no financial disclosures. This study was sponsored and funded by MTF. The Article Processing Charge was paid for by MTF.*

Supplemental digital content is available for this article. Clickable URL citations appear in the text.

can sequester and control the bioavailability of growth factors that modulate cellular responses by serving as a growth factor reservoir.[4,5,12] Apart from providing biological cues, the ECM imparts mechanical properties in the form of structural, tensile, and compressive support.[13,14] Its architecture influences material stiffness, which regulates cell behavior by affecting cytoskeletal reorganization and cell signaling,[15,16] whereas an open microstructure can facilitate host cell infiltration.[17] These native dermal properties can guide cell behavior and tissue remodeling in a wound care setting.

Exogenous scaffolds replace or replicate native ECM by restoring structural and functional requirements.[1,12,18] They also provide a barrier to protect wounds from infection and desiccation. Scaffold origins can be cellular or acellular and originate from biological, synthetic, or composite materials.[1,19] Although synthetic scaffolds are reproducible and uniform, they lack the biological advantages of native dermal matrices.[5,19] ADMs can be processed to preserve the dermal structure and leverage the dermal biology to reduce scarring and improve tissue regeneration.[2,20–22]

The structure of human dermis can be divided into 2 layers: papillary or superficial and reticular.[1] The fibrils present in the papillary dermis are smaller compared with the reticular dermis. When the papillary dermis is injured (superficial cut or burn), it can often regenerate without a scar. The reticular dermis is the deeper and thicker region composed of dense collagen fibers, elastin, and woven reticular fibers. These characteristics provide this region with strength, extensibility, and elasticity.[23] In a deep wound, this framework is missing, which can lead to scarring. By using an organized structure, this can coordinate new tissue repair and potentially address scarring.

ADM processing aims to remove cellular material to reduce immunogenicity and decontaminates or sterilizes the graft to limit disease transmission.[2,24] If not designed appropriately, however, the processing can negatively impact the endogenous matrix proteins and natural architecture that can hamper host cell integration and result in encapsulation and foreign body response.[25,26] Aseptic tissue processing utilizes gentle decontamination steps to ensure tissue safety, while preserving the matrix configuration.

In this study, we investigate the hypothesis that aseptically processed reticular dermal grafts provide a scaffold possessing biological and mechanical properties that can support wound healing. This unique deeper cut reticular dermis retains architectural elements (open structure), mechanical properties (elasticity, organized collagen and elastin), and key matrix proteins to support physiological cellular responses during regenerative remodeling.

MATERIALS AND METHODS

Tissue Procurement

Human dermal tissue was screened and recovered following industry standard guidelines. Human reticular ADMs (HR-ADMs; AlloPatch Pliable, Musculoskeletal Transplant Foundation, Edison, N.J.) was processed aseptically (Fig. 1) without terminal sterilization at Musculoskeletal Transplant Foundation (Edison, N.J.). The tissue was decellularized and disinfected with peracetic acid–based solution and every lot was assessed as per ⟨USP-71⟩ Sterility Tests. The papillary dermis was prepared in a similar method as a comparison. Both reticular and papillary layers were cut to final tissue specifications of 0.4–1.0 mm thick.

ADM Structure

Prehydrated papillary and reticular dermis samples (n = 3 donors) were fixed in 10% formalin, embedded in paraffin, sectioned into 5 μm thick cross-sections, and stained for hematoxylin and eosin (H&E) by Premier Laboratory, LLC (Boulder, Colo.).

Scanning electron microscopy (SEM) imaging was performed to visualize the microstructure of HR-ADM in comparison to papillary dermis (n = 3 donors). Samples were fixed in 10% formalin for 24 hours, rinsed with water twice for 15 minutes, and dehydrated in 50%, 70%, 80%, 95%, and 100% ethanol successively for 15 minutes each. These dry samples were coated under vacuum using

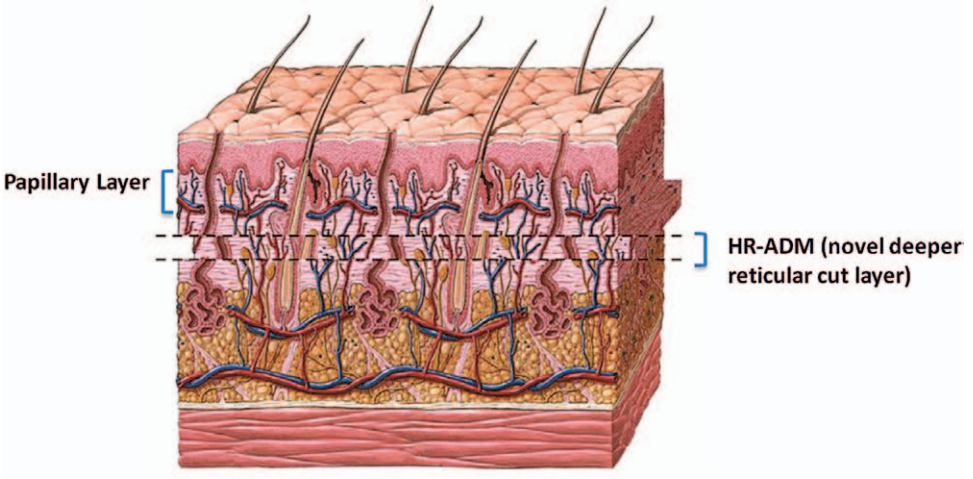

Fig. 1. HR-ADM, a novel deeper cut reticular dermis layer, present below the papillary dermis layer.

a Balzer MED 010 evaporator (Technotrade International, Manchester, NH) with platinum alloy to a thickness of 25 nm and immediately flash carbon coated under vacuum. Samples were examined in a JSM-5910 SEM (JEOL USA, Inc., Peabody, Mass.) at an accelerating voltage of 25 kV. Imaging was conducted at 250×.

The material porosity (n = 3 donors) was determined through gravimetric method assuming the material is close to density of collagen (1.34 g/cm^3), as collagen is the largest component of dermal tissue. The density of the tissue (using a ratio of dry and wet tissue densities) was calculated as per Loh and Choong.[27] The pore size range was evaluated by mercury intrusion porosimeter (Quantachrome, Fla.) using standard techniques. Mercury is forced into the dermal sample under high pressure through the porosimeter. The pressure needed to force mercury into the sample is inversely proportional to the pore size.

Biomechanical Characterization

Biomechanical properties of dermal tissue were evaluated using a MTS 858 Mini-Bionix tensile testing system (MTS, Eden Prairie, Minn.) with a calibrated 1 kN load cell. Dermal grafts (n = 3 donors) were cut into multiple specimens (4–12) using a custom punch shaped and sized to match the type V (microtensile testing) specimen specified by the American Society for Testing and Materials (ASTM) D638 guidelines for evaluating material properties (3.18 mm width; 0.4–1.0 mm thick). Sample thickness was measured and then loaded into tensile grips. Specimens were pulled under tensile load at a rate of 50.8 mm/min until failure. Ultimate tensile stress (UTS), Young's modulus, and the percentage elongation at break were examined and normalized to cross-sectional area.

Matrix Protein Characterization

Immunohistochemistry staining was performed at HistoTox Labs, Inc. (Boulder, Colo.). Operators were blinded to HR-ADMs (sample 1) and unprocessed reticular dermis (sample 2) for collagens I, III, IV, and VI and elastin. The levels of GAG and HA in HR-ADMs were compared with unprocessed reticular dermis (n = 3 donors). GAGs were quantified using the Blyscan GAG assay (Biocolor Life Science Assays; Carrickfergus, UK/Fisher Science, Houston, Tex.). Samples were extracted in papain (125 μg/mL in 0.1 M phosphate buffer) for 2 hours at 65°C and centrifuged (10,000 rpm; 10 minutes). The dye-binding assay was performed and absorbances were read at 656 nm. HA was quantified using an enzyme-linked immunosorbent assay (Corgenix, Broomfield, Colo.). Samples were extracted (24 hours, 4°C in 1 M sodium chloride and sodium bicarbonate solution), homogenized for 5 minutes in a bullet blender (Next Advance, N.Y.), and centrifuged (10,000 rpm; 10 minutes). Absorbances were read at 450 nm.

Enzymatic Degradation

HR-ADM samples were air dried overnight, weighed (21–25 mg), and rinsed in 0.9% saline solution. Samples (n = 3 donors) were then enzymatically digested (6 hours, 37°C water bath) in a collagenase type 1A (6.65 U/mL final enzyme solution; Sigma, St. Louis, Mo.) and thermolysin (15 U/mL final enzyme solution; Sigma, St. Louis, Mo.) solution in tricine buffer (pH 7.5). The filtered extract was mixed with ninhydrin (0.016 g/1 mL solution)–hydrindantin (0.0024 g/1 mL solution) (Sigma, St. Louis, Mo.) in ethylene glycol monoethyl solution and 4 N sodium acetate buffer (pH 5.5) that reacts with the released amino acids, producing a deep purple color proportional to the amount of peptides released. The standard curve was established with L-leucine (stock solution 2.0 mg/mL; Sigma, St. Louis, Mo.) and sample absorbances were read at 570 nm. The controls were crosslinked[28] and denatured dermis samples. Unprocessed dermal tissue was crosslinked (16 hours, room temperature) with 0.025% glutaraldehyde (Sigma, St. Louis, Mo.) solution, followed by a 2-hour rinse step to remove residual glutaraldehyde. The denatured condition (representing harsh chemical processing) was prepared by crosslinking as above and then boiling (at 100°C) the rinsed samples for 5 minutes. These samples were digested as stated above, reacted, and read at 570 nm.

Cell Behavior Characterization

Normal human dermal fibroblasts (NHDFs; Lonza, Walkersville, Md.) were cultured (0.2 million cells/7 mm disk) on HR-ADMs in fibroblast growth medium (FGM-2) (Lonza) at 37°C and 5% CO_2 in a humidified atmosphere. Cell attachment and matrix production were assessed over time (0, 7, 14 days). H&E, collagen IV, and fibronectin staining were performed by IHC World, LLC (Ellicott City, Md.), with standard histology techniques. Human umbilical vascular endothelial cells (HUVECs) were cultured (0.2 million cells/7 mm disk) on HR-ADMs to examine angiogenic capacity through tubular formation (CD31, AbCam, Cambridge, Mass.) and secretion of functional angiogenic factor, von Willebrand Factor (vWF; AbCam, Cambridge, Mass) on adhered cells through 4', 6-diamidino-2-phenylinadole (Life Technologies, Carlsbad, Calif) staining. Confocal imaging (Rutgers University, Piscataway, N.J.) was performed to visualize tubular network formation and vWF secretion.

Statistical Analysis

All values are reported as average and SD. A student t-test (unpaired) was used to compare mechanical evaluation of dermal tissue (HR-ADM versus papillary), and enzymatic degradation analysis (unprocessed dermis to HR-ADM, crosslinked and denatured), with $P < 0.05$ being considered significant.

RESULTS

Unique Feature of HR-ADM

H&E staining of HR-ADM revealed an open, uniform architecture (no orientation or polarity; Fig. 2). In contrast, the papillary graft was asymmetrical (epidermal-facing side was dense versus the open dermal-facing side), resulting in directionality (distinct orientation or polar-

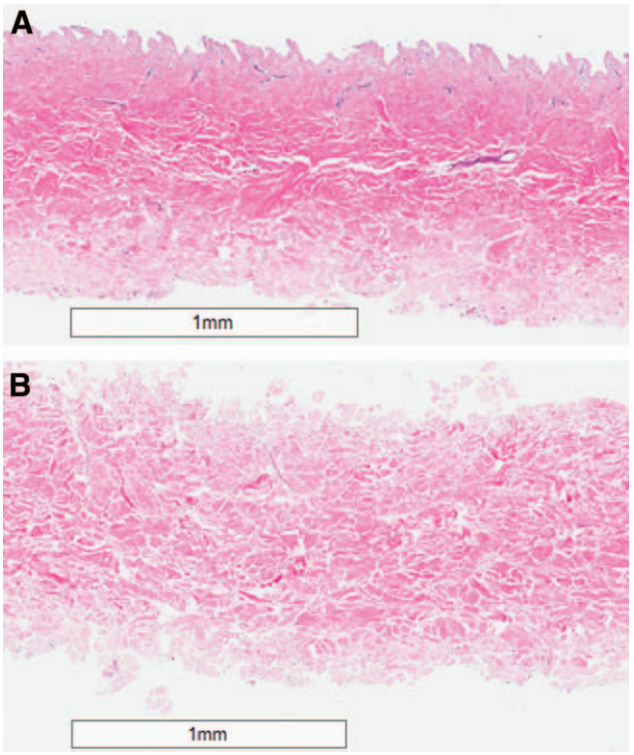

Fig. 2. A, Papillary Dermis is asymmetrical. B, HR-ADM is symmetrical. H&E revealed that the papillary dermis has an asymmetrical matrix structure, whereas the HR-ADM is symmetrical with a more uniform and open structure (magnification 2×). The papillary dermis is dense collagen on one side and loose collagen on the other side (distinct orientation present). The HR-ADM is uniform throughout and similar on both sides of the graft (no sidedness or orientation).

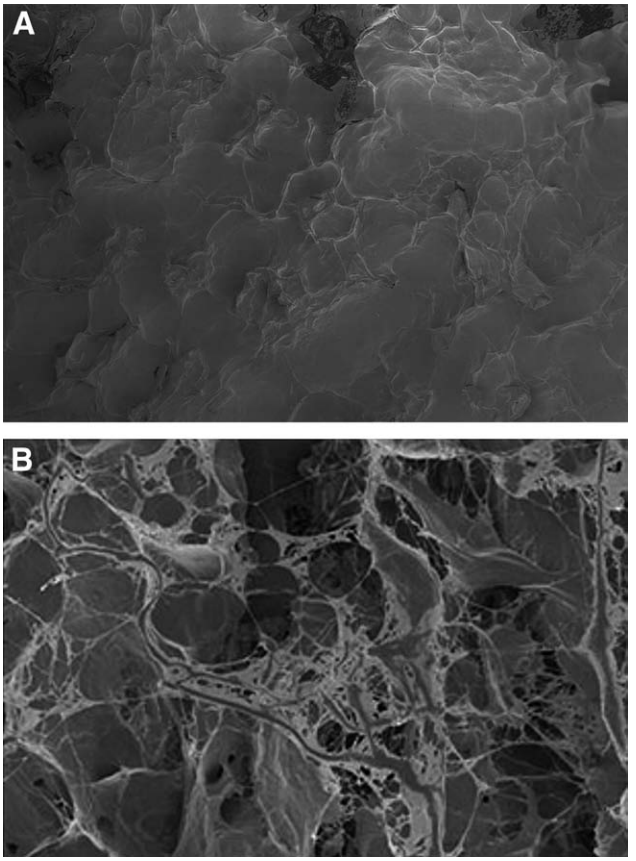

Fig. 3. A, Papillary Dermis. B, HR-ADM. SEM imaging displays the microstructure of HR-ADM and papillary dermis. The papillary dermal graft has a dense appearance at the epidermal facing side, whereas HR-ADM has open, porous appearance on the papillary facing side (magnification at 250×).

ity). Higher magnification (20×) images clearly demonstrated the consistent open, interconnected network of HR-ADM compared with the asymmetrical papillary dermis (**See PDF**, **Supplemental Digital Content 1**, which reveals distinct structural differences between papillary and reticular dermal structures, ***http://links.lww.com/PRSGO/A274***). Additionally, SEM imaging (Fig. 3) confirmed the open architecture present in HR-ADMs compared with papillary dermis. The porosity of HR-ADM was 88% ± 4% and of papillary dermis was 82% ± 6%. The pore size range as determined by mercury intrusion for HR-ADMs was 2.7–500 μm, whereas that determined for papillary dermis was 0.8–500 μm (Table 1). This open, interconnected network in HR-ADMs was seen in Figure 2, and this pore size range supports cell infiltration as evidenced in Figure 7.

Biomechanical Characterization

The HR-ADM thickness was 0.8 ± 0.2 mm (n = 4 donors; 4–8 samples/donor), whereas the papillary dermis thickness was 0.7 ± 0.1 mm (n = 3 donors; 8–12 samples/donor). HR-ADMs exhibited lower UTS values (7 ± 2 MPa) and Young's modulus (6 ± 1 MPa) compared with the papillary dermis UTS (14 ± 3 MPa) and Young's modulus (15 ± 3 MPa). HR-ADMs had significantly lower UTS (P = 0.03) and Young's modulus (P = 0.019) values compared with papillary dermis (Table 1). These lower biomechanical properties of HR-ADMs were similar to those reported for fetal porcine dermis as an elastic biomaterial comparison. The percentage elongation at break was significantly greater (P = 0.03) for HR-ADM (131% ± 15%) compared with papillary dermis (104% ± 2%), and is expected in an elastic scaffold. Generally,

Table 1. Biomechanical Properties of HR-ADM and Papillary Dermal Grafts

Material Properties	Papillary Dermis	HR-ADM	Fetal Porcine Dermis*
Porosity, %	82 ± 6	88 ± 4	Not reported
Pore size, μm	0.8–500	2.7–500	Not reported
Measured thickness, mm	0.7 ± 0.1	0.8 ± 0.2	Not reported
Ultimate tensile strength, MPa	14 ± 3	7 ± 2	2.1 ± 0.3
Young's modulus (stiffness), MPa	15 ± 3	6 ± 1	5.9 ± 1.5
% elongation at break, mm/mm	104 ± 2	131 ± 15	Not reported

The ultimate tensile strength and Young's modulus (stiffness) of HR-ADM and papillary dermis were compared to fetal porcine dermis.[37] HR-ADM demonstrates significantly lower tensile strength (P = 0.03) and Young's modulus (P = 0.019) and higher percentage elongation at break (P = 0.03) compared to papillary dermis.

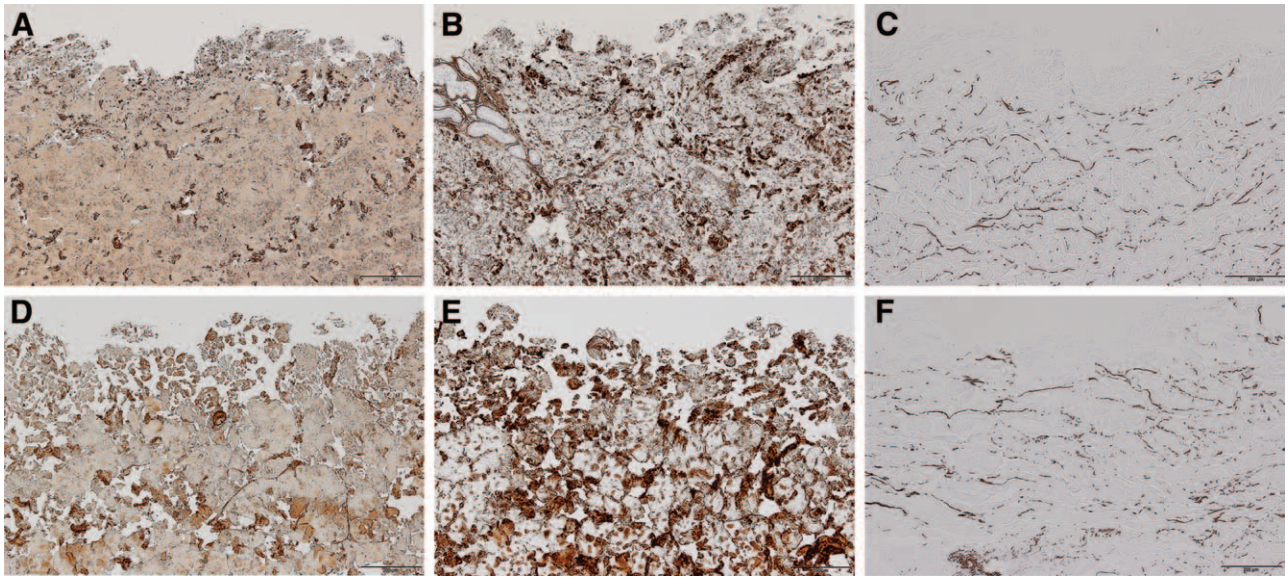

Fig. 4. Immunohistochemistry staining of unprocessed reticular dermis (A) Collagen I, (B) Collagen IV, (C) Elastin and HR-ADM (D) Collagen I, (E) Collagen IV, (F) Elastin. Aseptically processed HR-ADM revealed retention of collagen types I and VI and elastin as compared to unprocessed reticular dermis (magnification, 10×). All images were taken from the papillary facing side. Similar observations were found on the deep dermal facing side.

open porous scaffolds under tension align first, stretch, and break, whereas dense scaffolds, which have some orientation, load first and then break resulting in lower percentage elongation at break. Therefore, the biomechanical testing confirmed that the HR-ADMs are flexible structures, exhibiting low stiffness and increased elasticity.

Native ECM Components Preserved

Immunohistochemistry staining qualitatively revealed the retention of organized collagen types I and VI and elastin (Fig. 4) in unprocessed reticular dermis and HR-ADMs after aseptic processing (**See PDF**, **Supplemental Digital Content 2**, which demonstrates collagen III and IV retention, ***http://links.lww.com/PRSGO/A275***). Although there was some reduction in staining intensity for collagen III, the majority of the ECM components in HR-ADMs are similar to unprocessed tissue. Additionally, GAGs and HA were present and quantified in unprocessed reticular dermis (2.5±0.1 mg/g; 1000±88 μg/g) and retained in HR-ADMs (2.7±0.6 mg/g; 272±51 μg/g), respectively (Fig. 5). Although lower HA levels were present in the processed HR-ADM as compared with the unprocessed sample, a considerable amount of HA is retained. These critical ECM components provide an organized architecture to support cellular activities.

Enzymatic Degradation

To verify that aseptic processing preserves the native dermal components, enzymatic degradation studies examined the release of peptides in unprocessed and processed tissue samples along with controls (crosslinked, denatured dermis) representing process-altered tissue. Peptide release

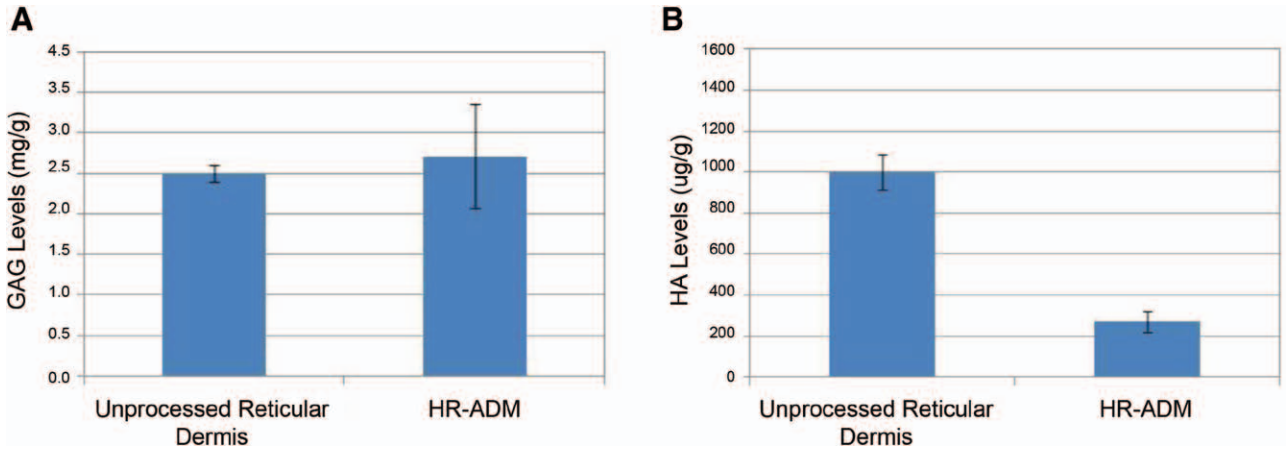

Fig. 5. A, Glycosaminoglycans (mg/g) and hyaluronic acid (μg/g; B) are present in aseptically processed HR-ADM compared to unprocessed reticular dermis.

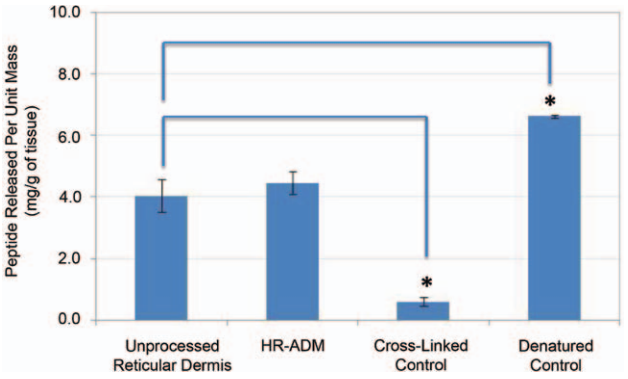

Fig. 6. Peptide release varied according to dermal processing methods. Aseptically processed HR-ADMs demonstrated similar peptide release profile compared to native, unprocessed reticular dermis. Crosslinked dermis with 0.025% glutaraldehyde[28] renders the matrix more resistant to degradation, with significantly (P = 0.004) lower peptide release, whereas denatured dermis yielded greater degradation of dermal components, with significantly (P = 0.013) greater peptide release.

for aseptically processed HR-ADMs (4.5±0.4 mg/g of tissue) was similar (no significant difference) to that for unprocessed reticular tissue (4.0±0.5 mg/g of tissue; Fig. 6). Crosslinking dermis resulted in significantly (P = 0.004) lower peptide (0.6±0.1 mg/g of tissue) release (resistance to degradation) due to the crosslinked collagen structure, whereas denatured dermis yielded significantly (P = 0.013) higher peptide (6.6±0.6 mg/g of tissue) release (degraded collagen); both reflecting altered tissue components. Therefore, aseptic processing preserves the native dermal components, whereas other processing methods may alter it.

In Vitro Cell Studies

Histological and confocal imaging demonstrated that both NHDFs and HUVECs readily attached to HR-ADMs. Histology analysis of NHDFs revealed cell attachment and infiltration into the graft (Fig. 7). Immunohistochemistry analysis confirmed fibroblasts secreted an abundance of collagen IV in a multilayered network on top and within the open HR-ADM network as early as day 7 (**See PDF**, **Supplemental Digital Content 3**, which displays fibronectin secretion and day 14 images, ***http://links.lww.com/PRSGO/A276***). HUVECs also readily attached (4', 6-diamidino-2-phenylinadole staining) with endothelial marker CD31, highlighting distinct, sustained tubular, network formation, and vWF, which is secreted by functional endothelial cells and confirming angiogenic capacity (Fig. 8). Similar observations were found on both sides of the HR-ADM. Both fibroblasts and endothelial cells are functional on HR-ADMs by attaching and secreting matrix proteins, which support granulation and angiogenic activities.

DISCUSSION

ADMs are used to protect the wound surface, maintain hydration, and provide a conducive microenvironment

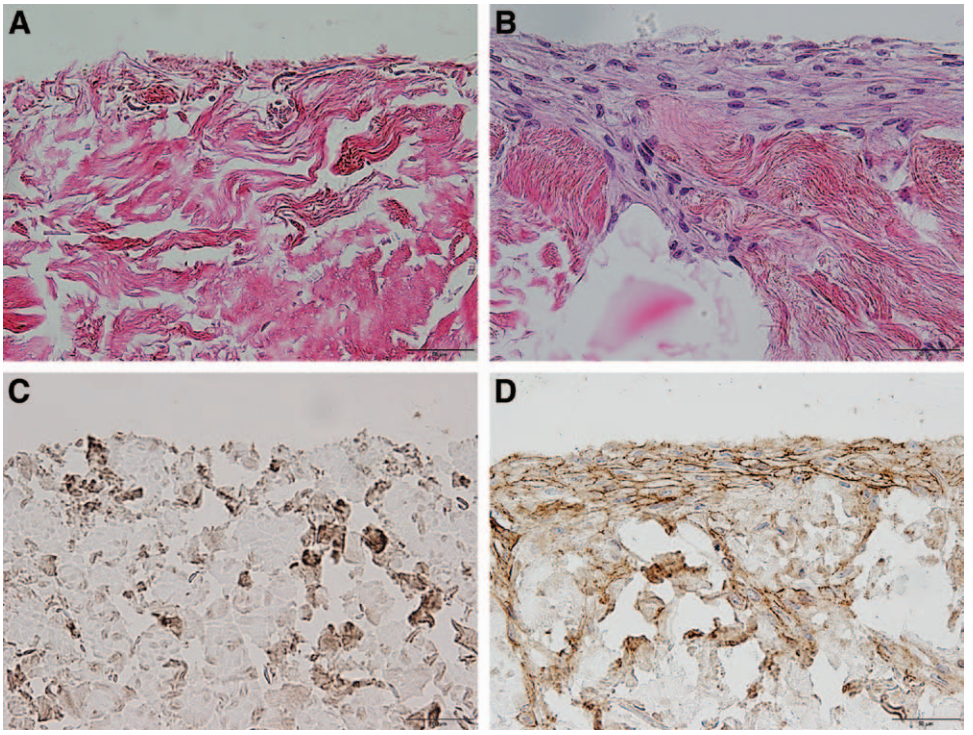

Fig. 7. H&E Histology demonstrated (A) HR-ADM alone and (B) NHDFs cultured on HR-ADMs at day 7 where cells readily attached and infiltrated within the graft (magnification 40×). Immunohistochemistry imaging revealed that (C) HR-ADM only and (D) NHDFs secreted an abundance of collagen IV on top and within the open, interconnected graft as early as day 7. Results were similar on both sides of the HR-ADM. These secreted ECM components support granulation activities.

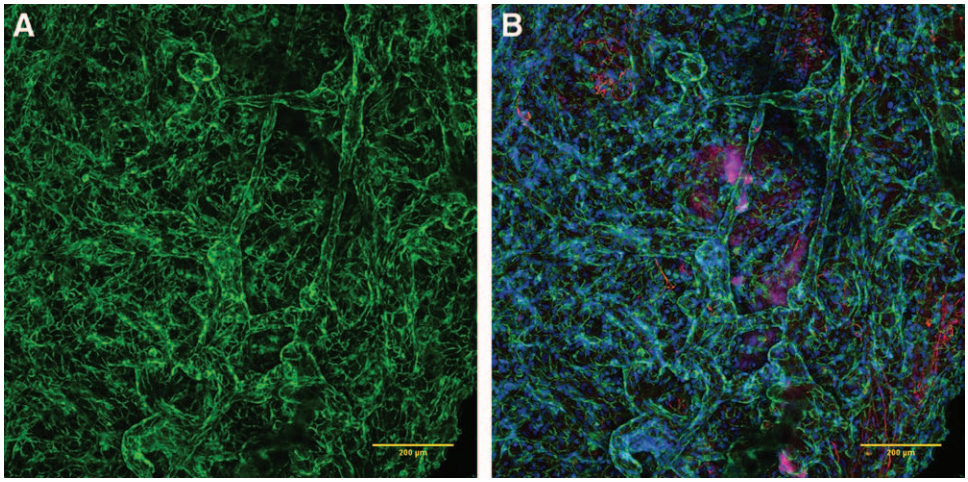

Fig. 8. Confocal imaging of HUVECs cultured for 10 days on HR-ADMs at 10× magnification. A, Endothelial cell marker, CD31 (green), revealed distinct, sustained tubular network formation. B, Adhered HUVECs shown by 4', 6-diamidino-2-phenylinadole staining (blue nuclei) have secreted vWF (red) which also verifies angiogenic capacity of functional endothelial cells. Similar observations were found on both sides of the HR-ADM.

for dermal repair and regeneration.[2,6,18,21,29] Traditionally, these matrices are obtained from the papillary dermal layer and are processed by methods that can alter the native dermal architecture and tissue quality, thereby impacting host engraftment and tissue remodeling. The novel dermal graft (HR-ADM) obtained from the deep reticular dermis layer used in this study was aseptically processed, and this preserved the native architecture and key ECM components that facilitate graft integration.

Histological analysis of the papillary dermis revealed an asymmetrical network (dense on one side, open on the other); this architectural polarity within the papillary region has been reported previously.[1] The heterogeneous nature can impact cell infiltration and native tissue remodeling. The novel HR-ADM provided a uniform, open network, ensuring a homogeneous framework. The absence of any graft asymmetry or orientation can be beneficial in the clinical setting, facilitating the ease of use.

It is well known that open scaffold architectures modulate cell–matrix interactions and augment cellular activities and newly formed tissue.[30,31] Increasing porosity can significantly improve cellular infiltration and tissue integration,[30] whereas the intrinsic mechanical properties (stiffness, elongation) can regulate cellular behavior (proliferation, cell–matrix integration).[32–34] This study demonstrated that HR-ADMs had an open, interconnected network with elastic biomechanical properties that are similar to fetal skin and significantly lower than papillary dermis. From literature, papillary dermis exhibited biomechanical properties which are in alignment with our study; similar Young's modulus (18.4 MPa) for an ADM,[35] obtained from papillary dermis, and UTS values (22 ± 8 MPa[36] and 13–30 MPa[13]) were also observed. In contrast, HR-ADMs behaved similarly to fetal porcine tissue having low biomechanical properties: UTS (2.1 ± 0.3 MPa) and Young's modulus (5.9 ± 1.5 MPa).[37] Exhibiting similar biomechanical properties to fetal porcine tissue may culminate in reduced scar formation.[37–39] As human wounds heal, the stiffness has shown to increase from 18 to 40 kPa,[40] indicating wound bed fibrosis and scarring.[41,42] Now, depending on clinical applications, different biomechanical properties are necessary. In the wound setting, graft strength is not critical, whereas the elasticity, flexibility, and conformability to the wound topography and irregular wound sizes are advantageous. Hence, HR-ADMs provide a promising elastic scaffold for wound repair.

This study also demonstrated that aseptic processing preserved ECM components important for wound healing, including collagens and elastin. They provide a stable, organized structure along with signaling cues that facilitate wound healing.[4,12] Collagens are instrumental in supporting the wound healing phases[8,22]; homing inflammatory cells[3,7]; supporting fibroblast attachment/granulation[10,43]; and facilitating keratinocyte migration.[44] Fetal fibroblasts have been shown to express more collagen III than collagen I and promote a more reticular deposition of fibers in a basket-weave orientation, which can assist in minimizing scar formation.[45,46] This type of reticular collagen network can help promote regeneration versus repair and minimize scarring; that is distinctly different from disorganized, parallel bundles of collagen that cause scarring.[38] Elastin provides scaffold elasticity and also mediates cellular activities by regulating the activity of TGFβs and its presence/organization minimizes scar formation.[47–49] Therefore, the preserved organized, basket-weave collagen and elastin structure present in HR-ADMs may promote regenerative healing.

GAGs and HA, which are important biological components for both adult and fetal wound healing,[20,50] are also retained in HR-ADMs. Exogenous addition of HA has reduced scar formation in adults by harnessing local growth factors and modulating cell behavior.[51,52] GAGs also have an effect on chronic inflammatory response and fibrotic encapsulation, which otherwise may progress to implant

failure or scarring.[53] GAGs and HA can influence the ECM structure, assembly, and hydration[38]; impact inflammation[50,51]; and foster granulation and protect cells from free-radical damage.[25] The retention of both GAGs and HA in HR-ADMs is predictive of clinical utility in facilitating wound healing.

These key biological ADM properties are beneficial to be retained through the processing steps to remove bioburden and minimize immunogenicity. Terminal sterilization and harsh chemical treatments can modify the scaffold structure and degradation characteristics by resident enzymes found in wounds.[54–56] Furthermore, these treatments can damage the collagen structure and other bioactive components, hampering cell adhesion and cell–ECM interactions.[54,55] Crosslinking agents (such as glutaraldehyde[28]) strengthen scaffold biomechanical properties; however, they reduce the ability of cell–matrix interactions by impairing the collagen structure and cell-binding sites, yielding poor clinical properties.[26] Consequently, tissue processing strategies must balance bioburden reduction and cell removal with maintenance of scaffold integrity. This study verified aseptic processing retained the native dermal components. Furthermore, enzymatic degradation of HR-ADM yielded similar peptide release compared with unprocessed tissue, whereas crosslinking or denaturing dermis significantly altered peptide release.

Further evidence that aseptic tissue processing preserved the native architecture and biological components comes from in vitro fibroblast and endothelial cell studies in HR-ADMs. The open architecture of HR-ADMs (2.7–500 μm pore size range) and retained ECM components supported cell attachment and infiltration. Both cell types readily attached and were functional on the HR-ADMs by secreting an abundance of new matrix proteins (collagen IV, fibronectin, vWF) on top and within the graft. The secreted matrix proteins are critical in supporting granulation and angiogenesis[4,5,57,58] and stimulate and guide other cellular responses.[10,59]

In summary, aseptically processed HR-ADMs provide a unique, biologically and mechanically advantageous scaffold for wound repair. The in vitro findings are supported by the clinical findings where HR-ADMs combined with standard of care performed significantly better than standard of care alone in the treatment of chronic diabetic foot ulcers.[60] Further in vitro studies are needed to characterize the cell behavior and functionality of these biologically and mechanically stable novel reticular dermal grafts in a chronic setting.

Anouska Dasgupta, PhD
Musculoskeletal Transplant Foundation
125 May Street
Edison, NJ 08837
E-mail: Anouska_Dasgupta@mtf.org

REFERENCES

1. Simpson DG. Dermal templates and the wound-healing paradigm: the promise of tissue regeneration. *Expert Rev Med Devices* 2006;3:471–484.
2. Kirsner RS, Bohn G, Driver VR, et al. Human acellular dermal wound matrix: evidence and experience. *Int Wound J.* 2015;12:646–654.
3. Clark RA, Ghosh K, Tonnesen MG. Tissue engineering for cutaneous wounds. *J Invest Dermatol.* 2007;127:1018–1029.
4. Schultz GS WA. Interactions between extracellular matrix and growth factors in wound healing. *Wound Repair Regen.* 2009;17:153–162.
5. Schultz GS, Davidson JM, Kirsner RS, et al. Dynamic reciprocity in the wound microenvironment. *Wound Repair Regen.* 2011;19:134–148.
6. Ruszczak Z. Effect of collagen matrices on dermal wound healing. *Adv Drug Deliv Rev.* 2003;55:1595–1611.
7. Mustoe T. Understanding chronic wounds: a unifying hypothesis on their pathogenesis and implications for therapy. *Am J Surg.* 2004;187:65S–70S.
8. Frantz C, Stewart KM, Weaver VM. The extracellular matrix at a glance. *J Cell Sci.* 2010;123(Pt 24):4195–4200.
9. Smith MM, Melrose J. Proteoglycans in normal and healing skin. *Adv Wound Care (New Rochelle)* 2015;4:152–173.
10. Midwood KS, Mao Y, Hsia HC, et al. Modulation of cell-fibronectin matrix interactions during tissue repair. *J Investig Dermatol Symp Proc.* 2006;11:73–78.
11. Chen WY, Abatangelo G. Functions of hyaluronan in wound repair. *Wound Repair Regen.* 1999;7:79–89.
12. Briquez PS, Hubell JA, Martino MM. Extracellular matrix-inspired growth factor delivery systems for skin wound healing. *Adv Wound Care (New Rochelle)* 2015;4:479–489.
13. Gallagher AJ, Ní Annaidh A, Bruyere K, et al. Dynamic tensile properties of human skin. *2012 IRCOBI Conference Proc.* 2012;IRC-12-59.
14. Engler AJ, Sweeney HL, Discher DE, et al. Extracellular matrix elasticity directs stem cell differentiation. *J Musculoskelet Neuronal Interact.* 2007;7:335.
15. Krieg T, Aumailley M. The extracellular matrix of the dermis: flexible structures with dynamic functions. *Exp Dermatol.* 2011;20:689–695.
16. Ingber D. Extracellular matrix and cell shape: potential control points for inhibition of angiogenesis. *J Cell Biochem.* 1991;47:236–241.
17. Mao Y, Schwarzbauer JE. Stimulatory effects of a three-dimensional microenvironment on cell-mediated fibronectin fibrillogenesis. *J Cell Sci.* 2005;118(Pt 19):4427–4436.
18. Turner NJ, Badylak SF. The use of biologic scaffolds in the treatment of chronic nonhealing wounds. *Adv Wound Care (New Rochelle)* 2014;4:490–500.
19. Gibson D, Cullen B, Legerstee R, et al. MMPs made easy. *Wounds Int.* 2009;1:1–6.
20. Wu Z, Tang Y, Fang H, et al. Decellularized scaffolds containing hyaluronic acid and EGF for promoting the recovery of skin wounds. *J Mater Sci Mater Med.* 2015;26:5322.
21. Reyzelman AM, Bazarov I. Human acellular dermal wound matrix for treatment of DFU: literature review and analysis. *J Wound Care* 2015;24:128;129–134.
22. Brett D. A review of collagen and collagen-based wound dressings. *Wounds* 2008;20:347–356.
23. Shukla A, Nandi P, Ranjan, M. Acellular dermis as a dermal matrix of tissue engineered skin substitute for burns treatment. *Ann Public Health Res.* 2015;2:3:1023.
24. Crapo PM, Gilbert TW, Badylak SF. An overview of tissue and whole organ decellularization processes. *Biomaterials* 2011;32:3233–3243.
25. Hodde J, Janis A, Ernst D, et al. Effects of sterilization on an extracellular matrix scaffold: part I. Composition and matrix architecture. *J Mater Sci Mater Med.* 2007;18:537–543.
26. Debels H, Hamdi M, Abberton K, et al. Dermal matrices and bioengineered skin substitutes: a critical review of current options. *Plast Reconstr Surg Glob Open* 2015;3:e284.
27. Loh QL, Choong C. Three-dimensional scaffolds for tissue engineering applications: role of porosity and pore size. *Tissue Eng Part B Rev.* 2013;19:485–502.

28. Duan X, Sheardown H. Dendrimer crosslinked collagen as a corneal tissue engineering scaffold: mechanical properties and corneal epithelial cell interactions. *Biomaterials* 2006;27:4608–4617.
29. Holmes C, Wrobel JS, Maceachern MP, et al. Collagen-based wound dressings for the treatment of diabetes-related foot ulcers: a systematic review. *Diabetes Metab Syndr Obes.* 2013;6:17–29.
30. Zhang YN, Avery RK, Vallmajo-Martin Q, et al. A highly elastic and rapidly crosslinkable elastin-like polypeptide-based hydrogel for biomedical applications. *Adv Funct Mater.* 2015;25:4814–4826.
31. Vogel V, Sheetz M. Local force and geometry sensing regulate cell functions. *Nat Rev Mol Cell Biol.* 2006;7:265–275.
32. You C, Wang X, Zheng Y, et al. Three types of dermal grafts in rats: the importance of mechanical property and structural design. *Biomed Eng Online* 2013;12:125.
33. Tomasek JJ, Gabbiani G, Hinz B, et al. Myofibroblasts and mechano-regulation of connective tissue remodelling. *Nat Rev Mol Cell Biol.* 2002;3:349–363.
34. Huang X, Yang N, Fiore VF, et al. Matrix stiffness-induced myofibroblast differentiation is mediated by intrinsic mechanotransduction. *Am J Respir Cell Mol Biol.* 2012;47:340–348.
35. Silver FH, Freeman JW, DeVore D. Viscoelastic properties of human skin and processed dermis. *Skin Res Technol.* 2001;7:18–23.
36. Ní Annaidh A, Bruyère K, Destrade M, et al. Characterization of the anisotropic mechanical properties of excised human skin. *J Mech Behav Biomed Mater.* 2012;5:139–148.
37. Zak M, Kuropka P, Kobielarz M, et al. Determination of the mechanical properties of the skin of pig foetuses with respect to its structure. *Acta Bioeng Biomech.* 2011;13:37–43.
38. Wilgus TA. Regenerative healing in fetal skin: a review of the literature. *Ostomy Wound Manage.* 2007;53:16–31; quiz 32–33.
39. Solon J, Levental I, Sengupta K, et al. Fibroblast adaptation and stiffness matching to soft elastic substrates. *Biophys J.* 2007;93:4453–4461.
40. Goffin JM, Pittet P, Csucs G, et al. Focal adhesion size controls tension-dependent recruitment of alpha-smooth muscle actin to stress fibers. *J Cell Biol.* 2006;172:259–268.
41. Achterberg VF, Buscemi L, Diekmann H, et al. The nano-scale mechanical properties of the extracellular matrix regulate dermal fibroblast function. *J Invest Dermatol.* 2014;134:1862–1872.
42. Aarabi S, Bhatt KA, Shi Y, et al. Mechanical load initiates hypertrophic scar formation through decreased cellular apoptosis. *FASEB J.* 2007;21:3250–3261.
43. Masci VL, Taddei AR, Gambellini G, et al. Ultrastructural investigation on fibroblast interaction with collagen scaffold. *J Biomed Mater Res A.* 2016;104:272–282.
44. Werner S, Krieg T, Smola H. Keratinocyte-fibroblast interactions in wound healing. *J Invest Dermatol.* 2007;127:998–1008.
45. Merkel JR, DiPaolo BR, Hallock GG, et al. Type I and type III collagen content of healing wounds in fetal and adult rats. *Proc Soc Exp Biol Med.* 1988;187:493–497.
46. Mast BA, Diegelmann RF, Krummel TM, et al. Scarless wound healing in the mammalian fetus. *Surg Gynecol Obstet.* 1992;174:441–451.
47. Halper J, Kjaer M. Basic components of connective tissues and extracellular matrix: elastin, fibrillin, fibulins, fibrinogen, fibronectin, laminin, tenascins and thrombospondins. *Adv Exp Med Biol.* 2014;802:31–47.
48. Broughton G 2nd, Janis JE, Attinger CE. Wound healing: an overview. *Plast Reconstr Surg.* 2006;117(7 Suppl):1e-S–32e-S.
49. Almine JF, Wise SG, Weiss AS. Elastin signaling in wound repair. *Birth Defects Res C Embryo Today* 2012;96:248–257.
50. Mast BA, Haynes JH, Krummel TM, et al. *In vivo* degradation of fetal wound hyaluronic acid results in increased fibroplasia, collagen deposition, and neovascularization. *Plast Reconstr Surg.* 1992;89:503–509.
51. Iocono JA, Ehrlich HP, Keefer KA, et al. Hyaluronan induces scarless repair in mouse limb organ culture. *J Pediatr Surg.* 1998;33:564–567.
52. Hu M, Sabelman EE, Cao Y, et al. Three-dimensional hyaluronic acid grafts promote healing and reduce scar formation in skin incision wounds. *J Biomed Mater Res B Appl Biomater.* 2003;67:586–592.
53. Zhou G, Niepel MS, Saretia S, et al. Reducing the inflammatory responses of biomaterials by surface modification with glycosaminoglycan multilayers. *J Biomed Mater Res A.* 2016;104:493–502.
54. Nataraj C, Ritter G, Dumas S, et al. Extracellular wound matrices: novel stabilization and sterilization method for collagen-based biologic wound dressings. *Wounds* 2007;19:148–156.
55. Matuska AM, McFetridge PS. The effect of terminal sterilization on structural and biophysical properties of a decellularized collagen-based scaffold; implications for stem cell adhesion. *J Biomed Mater Res B Appl Biomater.* 2015;103:397–406.
56. Cheung DT, Perelman N, Tong D, et al. The effect of gamma-irradiation on collagen molecules, isolated alpha-chains, and crosslinked native fibers. *J Biomed Mater Res.* 1990;24:581–589.
57. Sawicka KM, Seeliger M, Musaev T, et al. Fibronectin interaction and enhancement of growth factors: importance for wound healing. *Adv Wound Care (New Rochelle)* 2015;4:469–478.
58. Reinke JM, Sorg H. Wound repair and regeneration. *Eur Surg Res.* 2012;49:35–43.
59. Mao Y, Schwarzbauer JE. Fibronectin fibrillogenesis, a cell-mediated matrix assembly process. *Matrix Biol.* 2005;24:389–399.
60. Zelen CM, Orgill DP, Serena T, et al. A prospective, randomised, controlled, multicentre clinical trial examining healing rates, safety and cost to closure of an acellular reticular allogenic human dermis versus standard of care in the treatment of chronic diabetic foot ulcers. *Int Wound J.* 2016 Apr 12. doi: 10.1111/iwj.12600 [Epub ahead of print].